
Article:
Flores, C., Santos, M., Pereira, S.B. et al. (8 more authors) (2019) The alternative sigma factor SigF is a key player in the control of secretion mechanisms in Synechocystis sp. PCC 6803. Environmental Microbiology, 21 (1). pp. 343-359. ISSN 1462-2912

https://doi.org/10.1111/1462-2920.14465

Manuscript meant for *Environmental Microbiology*

The alternative sigma factor SigF is a key player in the control of secretion mechanisms in *Synechocystis* sp. PCC 6803

Carlos Flores[1,2,3], Marina Santos[1,2,3], Sara B. Pereira[1,2], Rita Mota[1,2], Federico Rossi[4], Roberto De Philippis[4], Narciso Couto[5,‡], Esther Karunakaran[5], Phillip C. Wright[5,§], Paulo Oliveira[1,2], Paula Tamagnini[1,2,6,*]

[1]i3S – Instituto de Investigação e Inovação em Saúde, Universidade do Porto, Porto, Portugal.

[2]IBMC – Instituto de Biologia Celular e Molecular, Universidade do Porto, Porto, Portugal.

[3]ICBAS – Instituto de Ciências Biomédicas Abel Salazar, Porto, Portugal.

[4]Department of Agrifood Production and Environmental Sciences, University of Florence, Florence, Italy.

[5]ChELSI Institute, Department of Chemical and Biological Engineering, University of Sheffield, Sheffield, UK.

[6]Faculdade de Ciências, Departamento de Biologia, Universidade do Porto, Porto, Portugal.

[*]For correspondence: Paula Tamagnini; Rua Alfredo Allen, 208, 4200-135, Porto, Portugal; E-mail. pmtamagn@ibmc.up.pt; Tel. +351 220 408 800.

[‡] Present address: Centre for Applied Pharmacokinetic Research, University of Manchester, Manchester, UK.

[§] Present address: Faculty of Science, Agriculture & Engineering, Newcastle University, Newcastle, UK.

Running title: SigF controls secretion in *Synechocystis*

Originality-Significance Statement

Cyanobacteria are important primary producers and therefore crucial ecological players in several environmental processes, such as the carbon and the nitrogen cycle. The interest on cyanobacterial secretion has been rising not only to understand the cell interaction with the extracellular environment (e.g. through biofilm formation, quorum sensing and motility), but also to implement efficient industrial systems based on cyanobacterial cell factories. Therefore, understanding the regulatory networks underlying cyanobacterial secretion becomes essential to extend the knowledge about these important physiological mechanisms and/or to manipulate them. Here, and for the first time, we associate the alternative sigma factor SigF with the control of cyanobacterial classical and non-classical secretion pathways and demonstrate that SigF has a major influence in production of extracellular polysaccharides (RPS), vesiculation and protein secretion, as well as in the maintenance of the cell envelope in *Synechocystis* sp PCC 6803. Moreover, a comprehensive study of SigF impact on *Synechocystis* physiology revealed its pleiotropic action and possible targets under SigF control, highlighting its importance for environmental adaptation. Furthermore, the *Synechocystis* knockout mutant Δ*sigF* emerges as a promising platform to study/manipulate RPS production and to obtain higher amounts of the extracellular polymer.

Summary

Cyanobacterial alternative sigma factors are crucial players in environmental adaptation processes, which may involve bacterial responses related to maintenance of cell envelope

and control of secretion pathways. Here, we show that the Group 3 alternative sigma factor F (SigF) plays a pleiotropic role in *Synechocystis* sp. PCC 6803 physiology, with a major impact on growth and secretion mechanisms, such as the production of extracellular polysaccharides, vesiculation and protein secretion. Although Δ*sigF* growth was significantly impaired, the production of released polysaccharides (RPS) increased 3 to 4-fold compared to the wild-type. Δ*sigF* exhibits also impairment in formation of outer-membrane vesicles (OMVs) and pili, as well as several other cell envelope alterations. Similarly, the exoproteome composition of Δ*sigF* differs from the wild-type both in amount and type of proteins identified. Quantitative proteomics (iTRAQ) and an *in silico* analysis of SigF binding motifs revealed possible targets/pathways under SigF control. Besides changes in protein levels involved in secretion mechanisms, our results indicated that photosynthesis, central carbon metabolism, and protein folding/degradation mechanisms are altered in Δ*sigF*. Overall, this work provided new evidences about the role of SigF on *Synechocystis* physiology and associates this regulatory element with classical and non-classical secretion pathways.

Introduction

RNA polymerase sigma factors play a major role in the regulation of bacterial acclimation processes and cell survival (Gruber and Gross, 2003; Feklístov *et al.*, 2014). This regulation occurs after the perception of environmental signals and subsequent orchestration of the replacement of one sigma factor by another in the RNA polymerase holoenzyme (Österberg *et al.*, 2011). These events trigger a change in gene expression pattern, producing multiple cellular responses and allowing the adaptation of the bacterial cell. Therefore, bacterial sigma factors have been emerging as new targets to engineer a wide range of

microorganisms (Tripathi *et al.*, 2014; Stensjö *et al.*, 2017). The vast majority of bacterial sigma factors belong to the so-called σ^{70} family, due to their similarities with the sigma factor 70 from *E. coli* (Feklístov *et al.*, 2014; Paget, 2015), but some members of a second family (σ^{54}) have also been identified in a restricted number of bacteria. Sigma factors belonging to the σ^{70} family are commonly divided in four different groups: i) Group 1-sigma factors, which are essential to cell viability and mainly related with the transcription of housekeeping genes; ii) Group 2-sigma factors, structurally similar to those of group 1, but considered non-essential in near optimal growth conditions; iii) Group 3-sigma factors, responsible for the expression of regulons assigned to the survival under stress and iv) Group 4-sigma factors, also named as sigma factors of extracytoplasmic function (ECFs), since they respond to signals that are generated outside of the cell or in the cell wall. The Groups 3 and 4 are the most diverse and they comprise sigma factors that coordinate processes responsible for the maintenance or modification of the cell envelope, through sporulation (Hilbert *et al.*, 2004), motility (Zhao *et al.*, 2007), adhesion (Claret *et al.*, 2007), protein secretion (Eichelberg and Galán, 2000), quorum sensing (Schuster *et al.*, 2004), formation of biofilm matrices (Rachid *et al.*, 2000) and others. These processes seem to be intrinsically related with the secretion capacity of the microorganism, which can be achieved through pathways dependent on membrane transporters (Costa *et al.*, 2015) or mediated by vesicles (Swechheimer and Kuehn, 2015; Roier *et al.*, 2016). These mechanisms need to be tightly regulated in order to provide the most appropriate bacterial response, and to be rapidly remodeled when cells are exposed to different environmental conditions (Marx *et al.*, 2009; Christie-Oleza *et al.*, 2015; Donia and Fischbach, 2015). Despite the available knowledge on the influence of sigma factors and the regulatory networks behind secretion in pathogenic bacteria (see for e.g. Vilches *et al.*, 2009;

Rutherford and Bassler, 2012), information about these complex mechanisms is still limited for other bacteria.

In cyanobacteria, all sigma factors described until now belong to the σ^{70} family, being divided in three main groups according to Imamura and Asayama (2009). In these organisms, the ECF sigma factors are either categorized as an additional group (Bell *et al.*, 2017) or as a subset of Group 3 (Imamura and Asayama, 2009). Cyanobacterial Group 3 sigma factors generally occur at relatively low levels at optimal physiological conditions, but they are crucial players in environmental adaptation (Imamura *et al.*, 2003). They seem to perform similar roles to their orthologues in other bacteria, regulating pathways that involve repair of the cell envelope (Bell *et al.*, 2017), production and secretion of polysaccharides (Yoshimura *et al.*, 2007) and other acclimation processes (Inoue-Sakamoto *et al.*, 2007; Srivastava *et al.*, 2017). The study of cyanobacterial sigma factors has been mostly performed using the model unicellular cyanobacterium *Synechocystis* sp. PCC 6803 (hereafter *Synechocystis*). *Synechocystis´* Group 3 alternative sigma factors comprise a sub-group of three ECF sigma factors (SigG - Slr1545; SigH - Sll0856; SigI - Sll0687) and SigF (Slr1564), being the latter the most phylogenetically divergent protein (Imamura *et al.*, 2003). In contrast with its counterparts, the physiological importance of SigF has been poorly understood. Previous studies reported that SigF is important for *Synechocystis* motility through the regulation of pili formation (Bhaya *et al.*, 1999) and in adaptive responses to salt stress conditions (Marin *et al.*, 2002). Furthermore, Asayama and Imamura (2008) suggested that SigF may display stringent promoter recognition, being able to auto-regulate its gene expression.

The main goal of this study was to evaluate the impact of SigF on *Synechocystis* sp. PCC 6803 physiology, unveiling possible targets and biosynthetic pathways that may be under

the control of this Group 3 sigma factor, which is the only one that is not categorized as having an extracytoplasmic function.

Results

Synechocystis ΔsigF *mutant exhibits growth impairment and a clumping phenotype*

In this work, we started by characterizing *Synechocystis* wild-type (sub-strain PCC-M; Huckauf *et al.*, 2000) and its Δ*sigF* mutant, kindly provided by Prof. Martin Hagemann (University of Rostock, Germany) The growth of Δ*sigF* mutant was compared to that of the wild-type strain by measuring the OD_{730nm}, the content in chlorophyll *a* (chl *a*) and by cell counting. The growth curves based on chl *a* measurements revealed a growth impairment of approximately 50% of the mutant compared to the wild-type. This result was corroborated by counting the number of cells (being the μg chl *a* per cell similar for both strains: wild type $3.11 \pm 0.12 \times 10^{-2}$ and Δ*sigF* $3.26 \pm 0.26 \times 10^{-2}$) (Fig.1), but not by the OD_{730nm} measurements (Fig. S1). This is most probably due to the higher turbidity of the medium derived from the accumulation of secreted products in the Δ*sigF* culture. The Δ*sigF* growth impairment could be partially rescued (about 40%) by complementation (Fig. S2). This partial rescue is most probably due to altered *sigF* expression levels, that can be explained by the use of a replicative plasmid (pSEVA351) containing the native *sigF* gene under the control of different regulatory elements (the P_{rbcL} promotor and the B0032 or RBS found upstream of *rbcL*; for more details see Supporting Information Experimental Procedures).

Besides the obvious impairment in growth, Δ*sigF* exhibited a striking macroscopic phenotype with the cells clumping under mild orbital shaking and sedimenting spontaneously without agitation at a much faster rate than the wild-type – overnight for the mutant and about 3 weeks for the wild-type (Fig. 2A and Fig. 2B). Moreover, after

centrifugation a much thicker layer of extracellular material could be observed above the pellet of Δ*sigF* (Fig. 2C). This extracellular material stained with Alcian Blue, a specific dye for acidic polysaccharides. Therefore, the Δ*sigF* mutant seems to be overproducing extracellular polymeric substances (EPS).

The* ΔsigF *mutant produces more and distinct EPS

Since it was possible to observe that the Δ*sigF* mutant produces more EPS than the wild-type, we pursued the characterization by measuring the amount of total carbohydrates, capsular polysaccharides – CPS, and polysaccharides released to the extracellular medium – RPS. The amount of total carbohydrates in the culture and the amount of RPS are approximately 2-fold and 3.5-fold higher in the Δ*sigF* culture compared to the wild-type, respectively (Fig. 3). For the complemented mutant, the amount of total carbohydrates is approximately 1.5-fold higher compared to the wild-type whereas the production of RPS increases only by 0.8-fold (Fig. S2). No significant differences were observed in terms of CPS.

The RPS were isolated from both the wild-type and the Δ*sigF* cultures (Fig. 4) and the differences observed were not limited to the amount of polymer produced, but also encompassed the monosaccharidic composition (Table 1).

Eleven different monosaccharides were detected in wild-type in contrast with ten in Δ*sigF* RPS, with the prevalence of glucose in both cases. In general, the isolated RPS are composed by three hexoses (glucose, mannose and galactose), two deoxyhexoses (rhamnose and fucose), three pentoses (xylose, arabinose and ribose), two amino sugars (glucosamine and galactosamine) and two acidic hexoses/uronic acids (glucuronic and galacturonic acids). Considerable differences were observed in the amount of almost all

monosaccharides, with the exception of mannose, rhamnose and xylose. *Synechocystis* Δ*sigF* mutant secretes a polymer enriched in hexoses compared to the wild-type. On the other hand, the amount of the other sugars decreases in Δ*sigF* RPS, with the exception of rhamnose. Furthermore, two uronic acids were detected in Δ*sigF* RPS, whereas in the RPS from the wild-type only glucuronic acid was detected but in higher amount than in Δ*sigF*.

The cell envelope and vesiculation capacity are altered in the* ΔsigF *mutant

During the isolation of the polymers, a difference in pigmentation of the RPS produced by wild-type and the Δ*sigF* mutant was observed (Fig. 4). Therefore, we decided to analyze the composition of the extracellular medium. The absorption spectra of the concentrated samples showed the characteristic absorption peaks of carotenoids for both strains, but the absorption levels were significantly higher for the wild-type (Fig. 5A). Since carotenoids are lipophilic molecules and thus embedded in lipid structures, the presence of lipopolysaccharides (LPS) and lipids were also investigated. In agreement with the previous results, the medium from *Synechocystis* wild-type culture contains larger amounts of lipids, as well as LPS compared to the Δ*sigF* mutant (Fig. 5B). Altogether, these observations suggest the presence of outer membrane vesicles (OMVs) in the extracellular medium, predominantly in the wild-type culture. These results were confirmed by negative staining transmission electron microscopy, with the micrographs of the Δ*sigF* mutant clearly showing an impaired vesiculation capacity compared to the wild-type (Fig. 6).

Moreover, impairment in pili formation was also observed in these micrographs (Fig. 6A), and this observation is in agreement with the absence of phototactic motility by Δ*sigF* (Fig. 6C). Furthermore, a dense amorphous layer, probably consisting of crippled EPS and/or LPS, was detected by transmission electron microscopy surrounding Δ*sigF* cells

(Fig. 6A and Fig. S3), containing structures that resemble protein aggregates (Fig. 6A and 6B).

Still regarding the cell envelope ultrastructure, other alterations could be detected in Δ*sigF*, namely the thickness of the peptidoglycan layer (Fig. S3) that is considerably thicker (10.9 ± 0.3 nm), compared to the wild-type (6.5 ± 0.4 nm). Additionally, the LPS profile of the outer membrane isolated from Δ*sigF* cells is distinct compared to the wild-type (Fig. S4).

The* ΔsigF *exoproteome differs from the wild-type

Since critical differences in the cell envelope and secretion of *Synechocystis* wild-type and Δ*sigF* were observed, their exoproteomes were also analyzed by SDS-polyacrylamide gel electrophoresis. Overall, the exoproteome of the Δ*sigF* mutant is remarkably different from the wild-type with proteins of lower molecular weight accumulating in higher amounts in Δ*sigF* (Fig. 7). Coomassie stained bands and/or gel portions were subjected to in-gel trypsin digestion followed by peptide identification by mass spectrometry. Peptides from 21 different proteins and belonging to the following four functional categories were detected (Table 2 and Table S2): 'Carbon metabolism' (5 proteins), 'Secretion & Membrane transporters' (4 proteins), 'Photosynthesis' (3 proteins) and 'Protein folding & degradation' (1 protein). The remaining proteins (about half of the ones identified) are categorized as 'unknown'. The predicted protein localization revealed that nearly half of the proteins identified are expected to be functionally active in the outer membrane or in the periplasmic space (Table S2). However, three proteins are predicted to be located in the cytoplasm: Sll1525 (PrK), Sll1029 (CcmK1) and Sll1028 (CcmK2), which are proteins involved in the CO_2 fixation mechanism in *Synechocystis*. Furthermore, three proteins

associated with thylakoid membranes were also detected in the exoproteomes: the phycobiliproteins, Sll1577 and Sll1578 (CpcA and CpcB phycocyanin subunits, respectively), and the allophycocyanin Slr2067 (ApcA). These three proteins accumulate in higher amounts in Δ*sigF* exoproteome. On the other hand, Sll1009 is accumulating in higher abundance in the wild-type exoproteome. This protein was shown to be glycosylated (data not shown), and although is being annotated as a FrpC its exact function remains to be elucidated. The proteins Slr0191 (SpoIID), Slr1751 (PrC) and Sll1525 (PrK) accumulated exclusively in the exoproteome of Δ*sigF*. In contrast, the Slr1452 (SbpA) involved in the sulphate transport appeared only in the wild-type exoproteome.

SigF has a pleiotropic action on* Synechocystis *physiology

To obtain a holistic perspective about the impact of SigF in *Synechocystis* physiology and to investigate the putative pathways and possible targets under the control of SigF, two different approaches were implemented: (i) The *in silico* analysis of putative SigF binding sites in *Synechocystis* gene promoter regions (Fig. 8) and (ii) A quantitative proteomic analysis (iTRAQ) of cell extracts from *Synechocystis* wild-type and Δ*sigF* (Fig. 9). The complete description of the genes or proteins obtained in both analyses is listed in Table S3 and Table S4, respectively.

For the analysis of the putative SigF binding sites (Fig. 8), the consensus sequences GGGTAAG and [C/T]AGGC [N10-30] GGGT[A/G][A/G][A/G] previously reported by Asayama and Imamura (2008) were searched in the whole genome of the *Synechocystis* substrain understudy, which was deposited by Trautmann *et al.* (2012). The hits retrieved were manually curated (see Experimental procedures) and a total of 110 genes were found with promoter regions displaying a putative SigF binding site. Nearly half of the genes

identified encode proteins with unknown function. The majority of the remaining genes encode proteins involved in the central carbon metabolism, including glycosyltransferases and proteins involved in CO_2 fixation and glycolysis. Furthermore, genes encoding proteins responsible for energy production and conversion (photosynthesis and oxidative phosphorylation), and proteins involved in secretion pathways (including the ones related to pilin secretion) are highly represented. Several genes encoding proteins important for sensing environmental stimuli and coordinating stress-related responses were also identified, namely kinases (e.g. Sll1770, Sll1525), sensors of two-component systems (e.g. Slr0302, Sll1672), other regulators (e.g. Slr1305, Slr1416), as well as proteins involved in protein folding and degradation (e.g. Slr0093, Sll1063, Sll0055). Moreover, various promoter regions of genes that encode oxidoreductases were identified as harboring putative SigF binding sites.

Regarding the quantitative proteomic analysis (iTRAQ), a total of 313 proteins (out of the 1654 identified and quantified) had significant fold changes in the *Synechocystis* Δ*sigF* cell extracts compared to the wild-type. In general, the distribution of these proteins by functional groups is similar to the distribution of the proteins encoded by genes retrieved in the analysis of putative SigF binding sites (Fig. 9A). Both analyses have 12 hits in common, which embody the most promising candidates of being directly regulated by SigF (Table 3). In the iTRAQ analysis, only 22% of the proteins identified are categorized as "unknown function", and several proteins are associated to cell envelope maintenance, in contrast to the SigF binding sites analysis. The mechanisms related with the basal energy production and conversion, mainly through photosynthesis and oxidative phosphorylation, seem to be strongly affected in the Δ*sigF* mutant. The levels of the main players in light harvesting, the antenna proteins from phycobilissomes, are higher in the mutant, which is

corroborated by the higher amount of phycocyanin content in Δ*sigF* cell extracts detected by absorption spectra analysis (Fig. S5). In contrast, the Psa proteins that constitute the photosystem I are in lower abundance in Δ*sigF*. Remarkably, plastocyanin has one of the lowest levels and cytochrome c6 the highest level in the entire iTRAQ analysis, which clearly shows that cytochrome c6 is a preferential route for the photosynthetic electron transport in Δ*sigF*. In terms of oxidative phosphorylation, the different subunits from the main players in this process are less abundant in Δ*sigF*, for e.g. the NADH dehydrogenase, succinate dehydrogenase/fumarate reductase and ATP synthetase (ATPase). Therefore, the photosynthetic activity of Δ*sigF* was evaluated to understand how changes in protein levels related to the main mechanisms of energy production and conversion could affect primary metabolism (Fig. S6). These changes seem to be responsible for a higher photosynthetic rate in Δ*sigF*, which increases when cells are exposed to high-light intensity. In addition, the respiratory activity during the dark period of Δ*sigF* growth is also significantly higher compared to the wild-type (Fig. S6).

In agreement with our previous results, a wide range of proteins involved in the carbon metabolism were differentially expressed in Δ*sigF* mutant, in processes such as glycolysis, pentose phosphate pathway and CO_2 fixation. The two subunits of RuBisCO, the major enzyme responsible for CO_2 fixation in *Synechocystis,* are in lower levels in Δ*sigF*. This was confirmed by Western blot using antibodies against the large subunit (RbcL), which revealed a significant reduction in the levels of RbcL of approximately 75% in Δ*sigF* compared to the wild-type (Fig. S6). Other proteins described to be involved in the inorganic carbon (Ci) uptake are also in lower abundance in Δ*sigF* (Table S4). However, several proteins involved in the reactions immediately after CO_2 fixation or Ci uptake are in higher abundance.

Translation was the functional category with the highest number of proteins in higher abundance in Δ*sigF*, which indicates a deregulation of translational mechanisms (Fig. 9B). Remarkably, Δ*sigF* displays a higher number of chaperones, proteases, heat-shock proteins and folding catalysts that may help the mutant to cope with abnormal translational events. Additionally, the number and abundance of this type of proteins in the mutant suggests that Δ*sigF* cells may be under stress. Following up on these observations, the redox defenses were also investigated (Fig. S7). Although the levels of ROS were slightly higher in Δ*sigF*, they were not statistically significant. The activity of the superoxide dismutase (SOD) was significantly higher in the mutant, but the catalase activity decreased approximately 50%, either detected by zymography or measured by spectrophotometric assays. The reduction of catalase activity is in agreement with the lower catalase abundance in Δ*sigF,* detected in the iTRAQ. Additionally, the spectrophotometric analysis of carotenoids revealed a reduction in the levels of these pigments of about 50% in the mutant (Fig. S5). However, a protein that binds specifically to carotenoids (Slr1963) is in higher abundance in Δ*sigF* (Table S4).

Regarding proteins that play a role in the biosynthesis of cell envelope components, Slr0776 (LpxD), one of the few proteins described as being involved in LPS biosynthesis, shows lower levels in the Δ*sigF* mutant. Moreover, other proteins that are known to be involved in lipid biosynthesis and with altered abundance in Δ*sigF*, are also expected to affect not only LPS formation but also vesiculation.

Alterations were also observed for several membrane transporters and proteins involved/or predicted to be involved in secretory pathways (e.g. Sll0616 – SecA). In the case of cell motility, not only the pilin and the pilin export and assembly machinery are in lower levels in Δ*sigF*, but other proteins involved in cell photo- and chemotaxis are also affected. The abundance of some regulators (e.g. Sll1626 - LexA) is also negatively

affected in Δ*sigF*, reflecting the importance of the indirect regulation and cross-talk between regulatory networks in the pleiotropic role of SigF.

Discussion

The results of the extensive characterization of the Δ*sigF* (*slr1564*) knockout mutant presented here clearly show that this Group 3 sigma factor F has a remarkable pleiotropic effect on the physiology of this *Synechocystis* sub-strain (PCC-M) under the conditions tested. We show, for the first time, a strong growth impairment and conspicuous phenotype for the Δ*sigF* mutant (Fig. 1 and 2). Earlier, this was not observed by Huckauf *et al.* (2000) but it is important to notice that the cells where grown in very different conditions, namely (i) the presence of NaCl, which induces the production of compatible solutes and generally reduces EPS production (Kirsch *et al.*, 2017) (ii) aeration with CO_2-enriched air, which provides an additional inorganic carbon supply and it is widely used to optimize cyanobacterial fitness (Zhang *et al.*, 2002; Kim *et al.*, 2010).

We also showed that the knockout of *sigF* leads to higher RPS production and total carbohydrate content (Fig. 3). The overproduction of RPS, strongly suggests a re-direction of energy and carbon fluxes towards RPS production, with a negative impact on the growth rate, as commonly observed for *Synechocystis* overproducing other carbon-rich compounds (Yoo *et al.*, 2007; Carpine *et al.*, 2017). In addition, no increase in the storage of other carbon reserves (e.g. glycogen) could be observed on the electron transmission micrographs of Δ*sigF* (Fig. S3). Earlier, another sigma factor (SigJ) was shown to be important for EPS production by the cyanobacterium *Anabaena* sp. PCC 7120, but in this strain the increase occurred only when *sigJ* was overexpressed (Yoshimura *et al.*, 2007). *Synechocystis* does not have J-type sigma factors, but a BLASTp® analysis (NCBI database) revealed that

Synechocystis SigF besides being closely related to *Anabaena´* SigF shares some similarity with *Anabaena´* SigJ, which is in agreement with the phylogenetic proximity between F and J sigma factor subtypes in cyanobacteria (Imamura *et al.*, 2003; Yoshimura *et al.*, 2007). The higher amount of RPS produced most probably play an important role in the establishment of the clumping phenotype displayed by the Δ*sigF* cells (Fig. 2). This has been reported for other bacterial and cyanobacterial strains in which EPS promote aggregation and embedment of the cells, which may work as a mechanism of self-shading with the polymers acting as protective molecules against light stress (Miranda *et al.*, 2017; Quijano *et al.*, 2017). Furthermore, according to Trautmann *et al.* (2012), this *Synechocystis* substrain has already the predisposition to exhibit a stress-induced clumping phenotype due to the truncation of genes encoding the proteins Sll1951 (hemolysin HlyA) and Slr1753 (surface protein), and here we show that this feature can be exacerbated by the absence of SigF.

Although the RPS produced by both *Synechocystis* wild-type and Δ*sigF* display features commonly found in other cyanobacterial RPS, such as the high number of monosaccharides and the prevalence of glucose (Pereira *et al.*, 2009; Rossi and Philippis, 2016), our results show that the quality of the polymer produced by Δ*sigF* is also distinct from the wild-type (Table 1). These differences may have an impact on the physical-chemical properties of the extracellular polymer such as the hydrophobicity (due to the lower amount of deoxyhexoses/pentoses in Δ*sigF*) or the anionic nature (due to the absence of galacturonic acid in the wild-type). These alterations also suggest that the basic steps of RPS production and central carbon metabolism are under SigF control, as reinforced by the altered levels of a high number of proteins involved in the photosynthesis and central carbon metabolism in Δ*sigF* compared to the wild-type (Fig. 9 and Table S4).

In contrast with the increase of RPS in Δ*sigF* cultures, other components of the extracellular milieu were found in lower levels, namely carotenoids, LPS and lipids (Fig. 5) These results suggest impaired vesiculation ability, which was further confirmed by TEM analysis (Fig. 6A and 6B). Several studies have reported an increase in the formation of bacterial outer membrane vesicles (OMVs) as a result of cell stress, being a mechanism of releasing damaged cellular material into the extracellular space and/or promote communication among neighbor cells, similar to a warning (McBroom and Kuehn, 2007, Gonçalves *et al.*, 2018). Although *Synechocystis* SigF is phylogenetically closest to *E. coli* FliA, in *E. coli* these events rely on different pathways regulated by SigE (Uniprot accession id P0AGB6; McBroom and Kuehn, 2007). Despite the decrease of OMVs formation, our results indicate that Δ*sigF* is under higher stress compared to the wild-type, as confirmed by the higher abundance of folding catalysts, chaperones and heat-shock proteins, which play a crucial role in protein quality control, maintenance of cell redox status and repair of cellular damages (Fig. 9 and Table S4). These proteins most probably function in alternative pathways to vesiculation in order to cope with accumulated damaged material. It is likely that the light intensity used here is one of the stress factors, since previous studies reported that SigF is crucial for light acclimation responses in *Synechocystis* (Huckauf *et al.*, 2000; Ogawa *et al.*, 2018). Furthermore, this hypothesis agrees with the higher amount of RPS and the strong clumping phenotype of the mutant, which are usual responses to light-induced stress (Miranda *et al.*, 2017; Quijano *et al.*, 2017). On the other hand, the lower levels/activities of some stress oxidative defenses in Δ*sigF* are either due to regulatory adjustments or to the energetic burden that they represent (Fig. S5 and S7). For example, it is likely that the reduction of carotenoid levels is related to the redirection of carbon skeletons to RPS overproduction, similar to what occurs in

Synechocystis mutants overproducing other carbon reserves such as glycogen or polyhydroxybutyrate - PHB (Antal *et al.*, 2016; Tokumaru *et al.*, 2018).

An absence of pili and of phototactic motility was also observed for Δ*sigF* (Fig. 6). This is in agreement with previous reports, describing SigF as the only sigma factor that regulates *pilA1* gene expression and consequent formation of pilin-like polypeptides in *Synechocystis* (Bhaya *et al.*, 1999; Asayama and Imamura, 2008). Bhaya *et al.* (1999) also described a "cell-surface aberration" surrounding Δ*sigF* cells formed by the accumulation of extracellular material enclosing protein aggregates, namely the main protein component of S-layer (HlyA). This structure is similar to the amorphous layer observed in our study and that is most likely formed by crippled EPS/LPS and other material resembling protein aggregates (Fig. 6A). In addition, other modifications were observed in sugar-rich cell envelope components of Δ*sigF* cells, such as a thicker peptidoglycan layer and alteration in the LPS profile on the O-antigen region (Fig. S3 and S4). These results can be explained by alterations in the sugar amount/type of saccharides linked to these structures, as previously reported for *Synechocystis* mutants with an altered central carbon metabolism (Mohamed *et al.*, 2005). The SigF importance in cell envelope maintenance was also reinforced by the iTRAQ results, showing that crucial proteins, such as Deg proteases, are in lower abundance in Δ*sigF* (Table S4). In addition, reduced levels of these proteins can increase cells sensitivity to light and oxidative stress, as well as result in protein secretion alterations (Barker *et al.*, 2006; Cheregi *et al.*, 2015). Indeed, the exoproteome of *Synechocystis* Δ*sigF* is remarkably different from the wild-type (Fig. 7 and Table 2). Among the 21 proteins identified, 13 were previously detected in *Synechocystis'* exoproteomes (Table S2). The variation in exoproteome composition among different studies may happen not only due to the growth conditions and method of isolation, but also depending on the substrain. Here

we describe the first exoproteome of a *Synechocystis* substrain without a S-layer due to the truncation of the HlyA protein (Trautmann *et al.*, 2012). In other *Synechocystis* substrains, HlyA accumulates extracellularly in such high amount that may hinder the identification of other proteins in the exoproteome samples. The phycocyanin subunits CpcA and CpcB are among the proteins that stand out in Δ*sigF* exoproteome suggesting possible cell lysis. Although CpcA is predicted to be secreted, these proteins (commonly found in thylakoids) are expected to be in lower abundance in the extracellular environment (Katoh, 1988; Gao *et al.*, 2014). In contrast, Sll1009 (unknown function) was found in higher abundance in the wild-type exoproteome. This protein is also predicted to be secreted and prone to suffer glycosylation (Gao *et al.*, 2014), as confirmed by us (data not shown). Since Δ*sigF* has an altered carbon metabolism, secretion alterations are expected for glycosylated proteins, that are usually predominant at the bacterial cell surface and in the extracellular space (Nothaft and Szymanski, 2010; Gao *et al.*, 2014). Moreover, we verify that the levels of several proteins involved in secretion mechanisms are altered in Δ*sigF* (Table S4). Among these, several components recently described as belonging to the TolC-mediated secretion mechanisms (Gonçalves *et al.*, 2018) are in higher abundance in Δ*sigF*. In contrast, proteins of the type 4 secretion system which are responsible for pilin assembly and secretion, are in lower abundance, indicating that the requirement of SigF for *Synechocystis* motility may not be exclusively due to the regulation of the *pilA* gene.

Regarding translation mechanisms, the higher levels of the different ribosome subunits in Δ*sigF* clearly indicate an overproduction of the ribosomal machinery, which was also recently observed in a Δ*sigBCDE* strain of *Synechocystis* sp. PCC 6803 lacking all Group 2 sigma factors (Koskinen *et al.*, 2018).

The two holistic approaches used to evaluate the impact of SigF in *Synechocystis* physiology, namely the iTRAQ quantitative proteomic analysis and the *in silico* search for SigF binding sites, confirmed the pleiotropic role of this sigma factor and a list of 12 gene candidates to be regulated by SigF emerged for further studies (Table 3). Two of these genes, *sll1694* (*hofG*/*pilA1*) and *sll0837* (*tadD*-like), were already reported as being SigF targets (Asayama and Imamura, 2008), which also reported that SigF regulates *sll0041* (*pixJ1*) expression (besides *sigF* autoregulation). In agreement, the proteins encoded by these three genes were found in lower abundance in Δ*sigF* (Table S4). Additionally, our results indicate that SigF can be indirectly controlling different pathways, since other regulators or proteins from sensory mechanisms have altered levels, and/or their encoding-genes present putative SigF binding motifs (Fig. 8 and 9; Tables S3 and S4). Our perspective is reinforced by the fact that several SigF bacterial orthologues were associated with the regulation of various processes that are intrinsically dependent on secretion pathways, such as motility (Ohnishi *et al.*, 1990; Claret *et al.*, 2007), quorum sensing (Schuster *et al.*, 2004) and morphological differentiation (Potuckova *et al*., 1995). Nevertheless, it is important to notice that the list of genes that are putatively regulated by SigF was generated by *in silico* analysis. Therefore, experimental validation studies are needed to confirm SigF specific binding and regulation.

In conclusion, the work presented here provides new evidence about the versatile role of SigF on *Synechocystis* physiology and its importance for environmental adaptation. The diversity of pathways and targets that are/could be under SigF influence also highlights how much is unknown about the regulatory networks involving alternative sigma factors. Nevertheless, SigF seems to have a particular importance in terms of cell envelope maintenance and control of classical and non-classical secretion pathways, being the first

regulatory element associated with secretion in *Synechocystis* (for a brief summary see Fig. 10). Moreover, *Synechocystis* Δ*sigF* emerges as a promising platform to study/manipulate EPS production and to obtain higher amounts of RPS. Interestingly, Δ*sigF* culture also presents the fastest *Synechocystis* spontaneous cell sedimentation described up to now, which is an important feature for industrial applications since it facilitates the harvesting of biomass and/or the recovery of secreted products.

Experimental Procedures

Bacterial strains and culture conditions

Synechocystis sp. PCC 6803 (sub-strain PCC-M, for details see Huckauf *et al.*, 2000; Trautmann *et al.* 2012), henceforth referred to as *Synechocystis* wild-type and the respective knockout mutant Δ*sigF* (both kindly provided by Prof. Martin Hagemann, University of Rostock, Germany) were grown in Erlenmeyer flasks containing BG11 media (Rippka *et al.*, 1979). Axenic cultures were incubated at 30 ^{o}C under a 12 h light (50 μE m^{-2} s^{-1}) / 12 h dark regimen, with orbital shaking at 150 rpm. Cultures of Δ*sigF* mutant were maintained in BG11 medium supplemented with kanamycin (100 μg ml^{-1}), while all experiments were performed in the absence of selective pressure.

DNA extraction and confirmation of mutant segregation

Cyanobacterial genomic DNA was extracted using a phenol/chloroform method (Tamagnini *et al*., 1997). Complete segregation of the mutants was confirmed by agarose gel electrophoresis of PCR amplification products using standard protocols (Sambrook and Russell, 2001) and Southern blot (oligonucleotides in Supporting Information Table S1). Southern blots were performed after digestion of genomic DNA with AseI (Thermo

Scientific). The DNA fragments were separated by electrophoresis on a 1% agarose gel and blotted onto Amersham HybondTM-N membrane (GE Healthcare). Probes were amplified by PCR and labeled using the DIG DNA labeling kit (Roche Diagnostics GmbH) according to manufacturer's instructions. Hybridization was done overnight at 60 ºC and digoxigenin labeled probes were detected by chemiluminescence using CPD-star (Roche Diagnostics GmbH) in a Chemi DocTM XRS+ Imager (Bio-Rad).

Growth assessment

Growth measurements were performed by monitoring the chlorophyll *a* content in cyanobacterial cultures as described by Meeks and Castenholz (1971) and by cell counting using Neubauer Chamber (Superior Marienfeld). Optical Density (OD) at 730 nm was also monitored spectrophotometrically (Shimadzu UVmini-1240, Shimadzu Corporation). All experiments were performed with three technical and three biological triplicates.

Determination of total carbohydrate content, RPS and CPS

The amount of total carbohydrates and released polysaccharides (RPS) in the cyanobacterial cultures were determined as previously reported in Mota *et al.* (2013). To isolate capsular polysaccharides (CPS), 5 ml of culture were centrifuged at 3857 *g* for 15 min, the pellet resuspended in 5 ml deionized water and boiled at 95 ºC during 15 min. The suspension was centrifuged at 3857 *g* and the supernatant used for CPS quantification using the phenol-sulfuric acid assay described in Dubois *et al.* (1956). All experiments were performed with three technical and three biological triplicates.

RPS extraction and Determination of monosaccharide composition

For RPS isolation, cultures were dialyzed (12–14 kDa of molecular weight cut-off; Medicell International Ltd.) against a minimum of 10 volumes of deionized water for 24 h with continuous stirring. The cells were removed by centrifugation at 12000 *g* during 15 min at 4 ^{o}C and the RPS were precipitated from the supernatant with two volumes of 96% cold ethanol. The suspension was centrifuged at 10000 *g* for 20 min at 15 ^{o}C, the pellet was resuspended in deionized water and lyophilized. The dried polymer was resuspended in deionized water and lyophilized again. To determine the monosaccharide composition, 5 mg of isolated RPS were hydrolyzed with 1 ml of 2 M trifluoroacetic acid (TFA) at 120 ºC for 1 h. Subsequently, samples were analyzed by ion exchange chromatography using an ICS-2500 ion chromatograph (Dionex Corporation) as described in Mota *et al.* (2013).

Light and Transmission electron microscopy (TEM)

For light microscopy, cells were observed directly using an Olympus X31 light microscope (Olympus). Micrographs were acquired with an Olympus DP25 camera using the Cellˆ B image software (Olympus). Staining with 0.5% (w/v) Alcian Blue in 3% (v/v) acetic acid was performed in 1:1 (culture:dye) ratio. For TEM, cells were collected, centrifuged and processed as described by Seabra *et al.* (2009), with the exception of the resin used that was EMBed-812 resin (Electron Microscopy Sciences). Ultrathin sections were examined using a JEM-1400Plus (Jeol). Negative staining was performed in 10 µl of cells or 500x concentrated media (diluted 1:100), mounted on formvar/carbon film coated mesh nickel grids (Electron Microscopy Sciences) and left standing for 2 min. The liquid in excess was removed with filter paper and 5 µl of 1% uranyl acetate was added on to the grids, and left standing for 10 s, after which liquid in excess was removed with filter paper.

Motility assays

Phototactic movement was examined on BG11 0.5% (w/v) agar plates (Bacto agar, Difco) supplemented with 10 mM TES and 10 mM glucose, where 15 µl of cell culture was spotted. The plates were half covered and exposed to unidirectional white light source.

Outer membrane isolation and Lipopolysaccharide (LPS) staining

Outer membranes were isolated as described by Simkovsky *et al.* (2012). The pellet was resuspended in 100 µl of 10 mM Tris-HCl, pH 8.0. Protease digested LPS samples were separated by electrophoresis on 12% SDS-PAGE (Bio-Rad) and stained using Pro-Q® Emerald 300 Lipopolysaccharide Gel Stain Kit (Molecular Probes) according to the manufacturer's instructions.

Concentration and analysis of extracellular medium

The medium from *Synechocystis* wild-type and Δ*sigF* cultures was isolated and concentrated as described in Oliveira *et al.* (2016). Concentrated samples were saved at -20 °C until further analysis. For the analysis of the pigments present in the medium, samples were diluted in 1:100 ratio and the absorption spectra in the visible light range of the extracts were measured at room temperature from 350 to 750 nm using Shimadzu UV-2401 PC spectrophotometer (Shimadzu Corporation). The relative abundance of carotenoids (CX index) was determined using carotenoids absorbance at 487 nm to the chl *a* absorbance at 663 nm ratio (Yang *et al.*, 2010). For LPS detection, concentrated medium samples were separated by gel electrophoresis on 12% SDS-polyacrylamide gels, which were stained as aforementioned. Subsequently, gels were incubated overnight with Sudan Black B solution

(0.5% (w/v) Sudan Black B in 17% (v/v) acetone and 12.5% (v/v) acetic acid) for lipids visualization.

Exoproteome analysis

The analysis of the exoproteomes was performed using concentrated medium samples. The protein concentration was measured using the BCA™ Protein Assay Kit (Pierce Biotechnology) and the iMark Microplate Absorbance Reader (Bio-Rad) according to the manufacturer's instructions, and 6 μg of protein were separated by electrophoresis on gradient 4–15% SDS-polyacrylamide gels (Bio-Rad) and visualized with colloidal Coomassie brilliant blue (Sigma). Stained bands or gel regions observed consistently across at least three biological replicates were further excised and processed for mass spectrometry analysis as previously described (Gomes *et al.*, 2013; Osório and Reis, 2013). Peptide mass spectra were acquired in reflector positive mode in the mass range of *m/z* 700–5000. Proteins were identified by Peptide Mass Fingerprint (PMF) approach with the Mascot software (v2.5.1, Matrix Science) using the UniProt protein sequence database for the taxonomic selection *Synechocystis* (2017_01 release). The predicted localization of the identified proteins was based on the ontology of their encoding-genes (GO annotations, EMBL-EBI database https://www.ebi.ac.uk/QuickGO/) and the PSORTb online tool (http://www.psort.org/psortb/).

In silico *consensus binding motif analysis*

Identification of putative gene promoter regions recognized by SigF was performed searching for the consensus binding motifs GGGTAAG, GGGT[A/G], [C/G]GGT[A/G][A/G/T], [C/T]AGGC [N10-30] GGGT[A/G][A/G][A/G] previously

reported by Asayama and Imamura (2008), in *Synechocystis* sp. PCC-M genome deposited by Trautmann *et al.* (2012). The sequences GGGT[A/G] and [C/G]GGT[A/G][A/G/T] are highly unspecific and retrieved a large number of hits, that were not considered for further analysis. For the remaining hits, a manual curation was performed in order to select only promoter regions that present a SigF binding motif within 300 bp upstream of the coding sequence. Description of the proteins encoded by the genes identified and their distribution into functional categories was based on CyanoBase (http://genome.microbedb.jp/cyanobase, Fujisawa *et al.*, 2016), Uniprot (http://www.uniprot.org/) and KEGG (Kyoto Encyclopedia of Genes and Genomes, http://www.genome.jp/kegg/) databases, and complemented with the information available in the literature.

iTRAQ experiment

The proteomes of *Synechocystis* wild-type and Δ*sigF* were analyzed by 8-plex isobaric tags for relative and absolute quantification (iTRAQ), using two biological and two technical replicates. The detailed description of the procedure can be found in the Supporting Information Experimental Procedures. The distribution into functional categories of the identified proteins was performed as described above.

Statistical analysis

Data were statistically analyzed in GraphPad Prism v7 (GraphPad Software) using an analysis of variance (ANOVA), followed by Bonferroni's multiple comparisons test.

Acknowledgments

This work was financed by FEDER - Fundo Europeu de Desenvolvimento Regional funds through the COMPETE 2020 - Operational Programme for Competitiveness and Internationalization (POCI); projects NORTE-01-0145-FEDER-000012 - Structured Programme on Bioengineering Therapies for Infectious Diseases and Tissue Regeneration, supported by Norte Portugal Regional Operational Programme (NORTE 2020), under the PORTUGAL 2020 Partnership Agreement; and by Portuguese funds through FCT – Fundação para a Ciência e a Tecnologia/Ministério da Ciência, Tecnologia e Ensino Superior in the framework of the project "Institute for Research and Innovation in Health Sciences" (POCI-01-0145-FEDER-007274) and grants SFRH/BD/99715/2014 (CF) and SFRH/BD/119920/2016 (MS). The authors thank Rui Fernandes, Francisco Figueiredo and Hugo Osório for their technical assistance. PCW and NC acknowledge the financial support from the European Union Seventh Framework Programme (FP7/2007-2013) under grant agreement number 308518 (CyanoFactory) and from BBSRC under grant number [BB/M012166/1]. PO was supported by Fundo Social Europeu and Programa Operacional Potencial Humano through the FCT Investigator grant IF/00256/2015, and by the POCI/FEDER-FCT grant POCI-01-0145-FEDER-029540.

The authors have no conflict of interest to declare.

References

Antal, T., Kurkela, J., Parikainen, M., Kårlund, A., Hakkila, K., Tyystjärvi, E., and Tyystjärvi, T. (2016) Roles of group 2 sigma factors in acclimation of the cyanobacterium *Synechocystis* sp. PCC 6803 to nitrogen deficiency. Plant Cell Physiol 57: 1309-1318.

Asayama, M., and Imamura, S. (2008) Stringent promoter recognition and autoregulation by the group 3 σ-factor SigF in the cyanobacterium *Synechocystis* sp. strain PCC 6803. Nucleic Acids Res 36: 5297.

Barker, M., de Vries, R., Nield, J., Komenda, J., and Nixon, P.J. (2006) The deg proteases protect *Synechocystis* sp. PCC 6803 during heat and light stresses but are not essential for removal of damaged D1 protein during the photosystem two repair cycle. J Biol Chem 281: 30347-30355.

Bell, N., Lee, J.J., and Summers, M.L. (2017) Characterization and in vivo regulon determination of an ECF sigma factor and its cognate anti-sigma factor in *Nostoc punctiforme*. Mol Microbiol 104: 179-194.

Bhaya, D., Watanabe, N., Ogawa, T., and Grossman, A.R. (1999) The role of an alternative sigma factor in motility and pilus formation in the cyanobacterium *Synechocystis* sp. strain PCC6803. Proc Natl Acad Sci U S A 96: 3188-3193.

Carpine, R., Du, W., Olivieri, G., Pollio, A., Hellingwerf, K.J., Marzocchella, A., and dos Santos, F.B. (2017) Genetic engineering of *Synechocystis* sp. PCC6803 for poly-β-hydroxybutyrate overproduction. Algal Res 25: 117-127.

Cheregi, O., Miranda, H., Gröbner, G., and Funk, C. (2015) Inactivation of the Deg protease family in the cyanobacterium *Synechocystis* sp. PCC 6803 has impact on the outer cell layers. J Photochem Photobiol B 152: 383-394.

Christie-Oleza, J.A., Armengaud, J., Guerin, P., and Scanlan, D.J. (2015) Functional distinctness in the exoproteomes of marine *Synechococcus*. Environ Microbiol 17: 3781-3794.

Claret, L., Miquel, S., Vieille, N., Ryjenkov, D.A., Gomelsky, M., and Darfeuille-Michaud, A. (2007) The flagellar sigma factor FliA regulates adhesion and invasion of Crohn disease-associated *Escherichia coli* via a cyclic dimeric GMP-dependent pathway. J Biol Chem 282: 33275-33283.

Costa, T.R., Felisberto-Rodrigues, C., Meir, A., Prevost, M.S., Redzej, A., Trokter, M., and Waksman, G. (2015) Secretion systems in Gram-negative bacteria: structural and mechanistic insights. Nat Rev Microbiol 13: 343.

Donia, M.S., and Fischbach, M.A. (2015) Small molecules from the human microbiota. Science 349: 1254766.

Dubois, M., Gilles, K.A., Hamilton, J.K., Rebers, P.A., and Smith, F. (1956) Colorimetric method for determination of sugars and related substances. Anal Chem 28: 350‑356.

Eichelberg, K., and Galán, J.E. (2000) The Flagellar Sigma Factor FliA (σ^{28}) regulates the expression of *Salmonella* genes associated with the centisome 63 type III secretion system. Infect Immun 68: 2735-2743.

Feklistov, A., Sharon, B.D., Darst, S.A., and Gross, C.A. (2014) Bacterial sigma factors: a historical, structural, and genomic perspective. Annual Rev Microbiol 68: 357-376.

Fujisawa, T., Narikawa, R., Maeda, S.I., Watanabe, S., Kanesaki, Y., Kobayashi, K., *et al.* (2016) CyanoBase: a large-scale update on its 20th anniversary. Nucleic Acids Res 45: D551-D554.

Gao, L., Huang, X., Ge, H., Zhang, Y., Kang, Y., Fang, L., *et al.* (2014) Profiling and Compositional Analysis of the Exoproteome of *Synechocystis* sp. PCC 6803. J Metabol Sys Biol 1: 8.

Gomes, C., Almeida, A., Ferreira, J.A., Silva, L., Santos-Sousa, H., Pinto-de-Sousa, J., *et al.* (2013) Glycoproteomic analysis of serum from patients with gastric precancerous lesions. J Proteome Res 12: 1454-1466.

Gonçalves, C.F., Pacheco, C.C., Tamagnini, P., and Oliveira, P. (2018) Identification of inner membrane translocase components of TolC-mediated secretion in the cyanobacterium *Synechocystis* sp. PCC 6803. Environ Microbiol 20: 2354–2369.

Gruber, T.M., and Gross, C.A. (2003) Multiple sigma subunits and the partitioning of bacterial transcription space. Annual Rev Microbiol 1: 441-466.

Hilbert, D.W., Chary, V.K., and Piggot, P.J. (2004) Contrasting effects of σ^{E} on compartmentalization of σ^{F} activity during sporulation of *Bacillus subtilis*. J Bacteriol 186: 1983-1990.

Huckauf, J., Nomura, C., Forchhammer, K., and Hagemann, M. (2000) Stress responses of *Synechocystis* sp. strain PCC 6803 mutants impaired in genes encoding putative alternative sigma factors. Microbiology 146: 2877-2889.

Imamura, S., and Asayama, M. (2009) Sigma factors for cyanobacterial transcription. Gene Regul Syst Bio 3: GRSB-S2090.

Imamura, S., Yoshihara, S., Nakano, S., Shiozaki, N., Yamada, A., Tanaka, K., *et al.* (2003) Purification, characterization, and gene expression of all sigma factors of RNA polymerase in a cyanobacterium. J Mol Biol 325: 857-872.

Inoue-Sakamoto, K., Gruber, T.M., Christensen, S.K., Arima, H., Sakamoto, T., and Bryant, D.A. (2007) Group 3 sigma factors in the marine cyanobacterium *Synechococcus* sp. strain PCC 7002 are required for growth at low temperature. J Gen Appl Microbiol 53: 89-104.

Katoh, T. (1988) Phycobilisome Stability. In Methods in enzymology. Academic Press, pp. 313-318.

Kim, H.W., Vannela, R., Zhou, C., Harto, C., and Rittmann, B.E. (2010) Photoautotrophic nutrient utilization and limitation during semi-continuous growth of *Synechocystis* sp. PCC6803. Biotechnol Bioeng 106: 553-563.

Kirsch, F., Pade, N., Klähn, S., Hess, W.R., and Hagemann, M. (2017) The glucosylglycerol-degrading enzyme GghA is involved in acclimation to fluctuating salinities by the cyanobacterium *Synechocystis* sp. strain PCC 6803. Microbiology 163: 1319-1328.

Koskinen, S., Hakkila, K., Kurkela, J., Tyystjärvi, E., and Tyystjärvi, T. (2018) Inactivation of group 2 σ factors upregulates production of transcription and translation machineries in the cyanobacterium *Synechocystis* sp. PCC 6803. Sci Rep 8: 10305.

Marin, K., Huckauf, J., Fulda, S., and Hagemann, M. (2002) Salt-dependent expression of glucosylglycerol-phosphate synthase, involved in osmolyte synthesis in the cyanobacterium *Synechocystis* sp. strain PCC 6803. J Bacteriol 184: 2870-2877.

Marx, J.G., Carpenter, S.D., and Deming, J.W. (2009) Production of cryoprotectant extracellular polysaccharide substances (EPS) by the marine psychrophilic bacterium *Colwellia psychrerythraea* strain 34H under extreme conditions. Can J Microbiol 55: 63-72.

McBroom, A.J., and Kuehn, M.J. (2007) Release of outer membrane vesicles by Gram-negative bacteria is a novel envelope stress response. Mol Microbiol 63: 545-558.

Meeks, J.C., and Castenholz, R.W. (1971) Growth and photosynthesis in an extreme thermophile, *Synechococcus lividus* (Cyanophyta). Arch Mikrobiol 78: 25-41.

Miranda, H., Immerzeel, P., Gerber, L., Hörnaeus, K., Lind, S.B., Pattanaik, B., *et al.* (2017) Sll1783, a monooxygenase associated with polysaccharide processing in the unicellular cyanobacterium *Synechocystis* PCC 6803. Physiol Plant 161: 182-195.

Mohamed, H.E., Van De Meene, A.M., Roberson, R.W., and Vermaas, W.F. (2005) Myxoxanthophyll is required for normal cell wall structure and thylakoid organization in the cyanobacterium *Synechocystis* sp. strain PCC 6803. J Bacteriol 187: 6883-6892.

Mota, R., Guimarães, R., Büttel, Z., Rossi, F., Colica, G., Silva, C.J., *et al.* (2013) Production and characterization of extracellular carbohydrate polymer from *Cyanothece* sp. CCY 0110. Carbohydr Polym 92: 1408-1415.

Nothaft, H., and Szymanski, C.M. (2010) Protein glycosylation in bacteria: sweeter than ever. Nat Rev Microbiol 8: 765-778.

Ogawa, K., Yoshikawa, K., Matsuda, F., Toya, Y., and Shimizu, H. (2018) Transcriptome analysis of the cyanobacterium *Synechocystis* sp. PCC 6803 and mechanisms of photoinhibition tolerance under extreme high light conditions. J Biosci Bioeng https://doi.org/10.1016/j.jbiosc.2018.05.015.

Ohnishi, K., Kutsukake, K., Suzuki, H., and Iino, T. (1990) Gene fliA encodes an alternative sigma factor specific for flagellar operons in *Salmonella typhimurium*. Mol Gen Genet 221: 139-147.

Oliveira, P., Martins, N.M., Santos, M., Pinto, F., Büttel, Z., Couto, N.A., *et al.* (2016) The versatile TolC-like Slr1270 in the cyanobacterium *Synechocystis* sp. PCC 6803. Environ Microbiol 18: 486-502.

Osorio, H., and Reis, C.A. (2013) Mass Spectrometry Methods for Studying Glycosylation in Cancer. In Mass Spectrometry Data Analysis in Proteomics. Matthiesen, R. (ed.). Totowa, New Jersey: Humana Press, pp. 301-316.

Österberg, S., Peso-Santos, T.D., and Shingler, V. (2011) Regulation of alternative sigma factor use. Annual Rev Microbiol 65: 37-55.

Paget, M.S. (2015) Bacterial sigma factors and anti-sigma factors: structure, function and distribution. Biomolecules 5: 1245-1265.

Pereira, S., Zille, A., Micheletti, E., Moradas-Ferreira, P., De Philippis, R., and Tamagnini, P. (2009) Complexity of cyanobacterial exopolysaccharides: composition, structures, inducing factors and putative genes involved in their biosynthesis and assembly. FEMS Microbiol Rev 33: 917-941.

Potuckova, L., Kelemen, G.H., Findlay, K. C., Lonetto, M.A., Buttner, M.J. and Kormanec, J. (1995) A new RNA polymerase sigma factor, sigma F, is required for the late stages of morphological differentiation in *Streptomyces* spp. Mol Microbiol 17: 37-48.

Quijano, G., Arcila, J.S., and Buitrón, G. (2017) Microalgal-bacterial aggregates: applications and perspectives for wastewater treatment. Biotechnol Adv 35: 772-781.

Rachid, S., Ohlsen, K., Wallner, U., Hacker, J., Hecker, M., and Ziebuhr, W. (2000) Alternative Transcription Factor σ^B Is Involved in Regulation of Biofilm Expression in a *Staphylococcus aureus* Mucosal Isolate. J Bacteriol 182: 6824-6826.

Rippka, R., Deruelles, J., Waterbury, J.B., Herdman, M., and Stanier, R.Y. (1979) Generic assignments, strain histories and properties of pure cultures of cyanobacteria. Microbiology 111: 1-61.

Roier, S., Zingl, F.G., Cakar, F., and Schild, S. (2016) Bacterial outer membrane vesicle biogenesis: a new mechanism and its implications. Microb Cell 3: 257.

Rossi, F., and De Philippis, R. (2016) Exocellular polysaccharides in microalgae and cyanobacteria: chemical features, role and enzymes and genes involved in their biosynthesis. In The physiology of microalgae. Springer, pp. 565-590.

Rutherford, S.T., and Bassler, B.L. (2012) Bacterial quorum sensing: its role in virulence and possibilities for its control. Cold Spring Harb Perspect Med 2: a012427.

Sambrook, J., and Russell, D.W. (2001) Molecular cloning: a laboratory manual, 3rd edn. New York, USA: Cold Spring Harbor Laboratory Press.

Schuster, M., Hawkins, A.C., Harwood, C.S., and Greenberg, E.P. (2004) The *Pseudomonas aeruginosa* RpoS regulon and its relationship to quorum sensing. Mol Microbiol 51: 973-985.

Schwechheimer, C., and Kuehn, M.J. (2015) Outer-membrane vesicles from Gram-negative bacteria: biogenesis and functions. Nat Rev Microbiol 13: 605.

Seabra, R., Santos, A., Pereira, S., Moradas-Ferreira, P., and Tamagnini, P., (2009) Immunolocalization of the uptake hydrogenase in the marine cyanobacterium *Lyngbya majuscula* CCAP 1446/4 and two *Nostoc* strains. FEMS Microbiol Lett 292: 57–62.

Simkovsky, R., Daniels, E.F., Tang, K., Huynh, S.C., Golden, S.S., and Brahamsha, B. (2012) Impairment of O-antigen production confers resistance to grazing in a model amoeba–cyanobacterium predator–prey system. Proc Natl Acad Sci U S A 109: 16678-16683.

Srivastava, A., Brilisauer, K., Rai, A.K., Ballal, A., Forchhammer, K., and Tripathi, A.K. (2017) Down-Regulation of the Alternative Sigma Factor SigJ Confers a Photoprotective Phenotype to *Anabaena* PCC 7120. Plant Cell Physiol 58: 287-297.

Stensjö, K., Vavitsas, K., and Tyystjärvi, T. (2017) Harnessing transcription for bioproduction in cyanobacteria. Physiol Plant 162: 148-155.

Tamagnini, P., Troshina, O., Oxelfelt, F., Salema, R., and Lindblad, P. (1997) Hydrogenases in *Nostoc* sp. Strain PCC 73102, a Strain Lacking a Bidirectional Enzyme. Appl Environ Microbiol 63: 1801-1807.

Tokumaru, Y., Uebayashi, K., Toyoshima, M., Osanai, T., Matsuda, F., and Shimizu, H. (2018) Comparative Targeted Proteomics of the Central Metabolism and Photosystems in SigE Mutant Strains of *Synechocystis* sp. PCC 6803. Molecules 23: 1051.

Trautmann, D., Voß, B., Wilde, A., Al-Babili, S., and Hess, W.R. (2012) Microevolution in cyanobacteria: re-sequencing a motile substrain of *Synechocystis* sp. PCC 6803. DNA Res 19: 435-448.

Tripathi, L., Zhang, Y., and Lin, Z. (2014) Bacterial sigma factors as targets for engineered or synthetic transcriptional control. Front Bioeng Biotechnol 2: 33.

Vilches, S., Jimenez, N., Tomás, J.M., and Merino, S. (2009) *Aeromonas hydrophila* AH-3 type III secretion system expression and regulatory network. Appl Environ Microbiol 75: 6382-6392.

Yang, D., Qing, Y., and Min, C. (2010) Incorporation of the chlorophyll d-binding light-harvesting protein from *Acaryochloris marina* and its localization within the photosynthetic apparatus of *Synechocystis* sp. PCC6803. Biochim Biophys Acta 1797: 204-211.

Yoo, S.H., Keppel, C., Spalding, M., and Jane, J.L. (2007) Effects of growth condition on the structure of glycogen produced in cyanobacterium *Synechocystis* sp. PCC6803. Int J Biol Macromol 40: 498-504.

Yoshimura, H., Okamoto, S., Tsumuraya, Y., and Ohmori, M. (2007) Group 3 sigma factor gene, *sigJ*, a key regulator of desiccation tolerance, regulates the synthesis of extracellular polysaccharide in cyanobacterium *Anabaena* sp. strain PCC 7120. DNA Res 14: 13-24.

Zhang, K., Kurano, N., and Miyachi, S. (2002) Optimized aeration by carbon dioxide gas for microalgal production and mass transfer characterization in a vertical flat-plate photobioreactor. Bioprocess Biosyst Eng 25: 97-101.

Zhao, K., Liu, M., and Burgess, R.R. (2007) Adaptation in bacterial flagellar and motility systems: from regulon members to 'foraging'-like behavior in *E. coli*. Nucleic Acids Res 35: 4441-4452.

Table Legends

Table 1. Monosaccharidic composition of the RPS obtained from *Synechocystis* wild-type and Δ*sigF* cultures expressed as molar %.

Table 2. List of proteins identified in the exoproteomes of *Synechocystis* sp. PCC 6803 wild-type (wt) and Δ*sigF* mutant by mass spectrometry.

Table 3. List of proteins displaying significant fold changes in *Synechocystis* Δ*sigF* compared to the wild-type (A and B are the two iTRAQ studies), encoded by genes displaying putative SigF binding motifs in their promoter regions.

Figure Legends

Fig. 1. Growth curves of *Synechocystis* sp. PCC 6803 wild-type (wt) and Δ*sigF* mutant. Growth was monitored by measuring the chlorophyll *a* (chl *a*) content and by counting the number of cells. Cells were grown in BG11 at 30 ^{o}C under a 12 h light (50 µE m^{-2} s^{-1}) / 12 h dark regimen, with orbital shaking at 150 rpm. Experiments were made in triplicate and the statistical analysis is presented for the last time point (**** p value ≤ 0.0001).

Fig. 2. *Synechocystis* sp. PCC 6803 wild-type (wt) and Δ*sigF* mutant phenotypes. **A.** Cultures after dialysis, showing the clumping of the mutant cells. **B.** Batch cultures depicting the higher rate of spontaneous sedimentation of Δ*sigF*. **C.** Centrifuged cultures where it is possible to observe the higher amount of EPS produced by the Δ*sigF* mutant compared to the wt, and light micrographs from the Δ*sigF* culture (**I** and **II**), with the EPS stained with Alcian Blue (**II**).

Fig. 3. Total carbohydrates, released and capsular polysaccharides of *Synechocystis* wild-type and Δ*sigF*. The values are expressed as mg of carbohydrates per mg of chlorophyll *a* (chl *a*). Cultures were grown in BG11 at 30 ^{o}C under a 12 h light (50 µE m^{-2} s^{-1}) / 12 h dark

regimen, with orbital shaking at 150 rpm. Experiments were made in triplicate and the statistical analysis is presented for the last time point (**** p value ≤ 0.0001). RPS: released polysaccharides, CPS: capsular polysaccharides.

Fig. 4. Purified lyophilized RPS obtained from *Synechocystis* wild-type and Δ*sigF* cultures.

Fig. 5. Analysis of concentrated medium from *Synechocystis* wild-type (wt) and Δ*sigF* cultures. **A.** Absorption spectra of the 500x concentrated medium, with arrows indicating the characteristic carotenoids peaks (upper panel) and quantification of the relative abundance of carotenoids - CX index (lower panel) (**** p value ≤ 0.0001). **B**. Lipopolysaccharides (LPS) profile analyzed by SDS-polyacrylamide gel electrophoresis and stained with Pro-Q® Emerald 300 lipopolysaccharide (upper left panel). The gel was subsequently stained with Sudan Black B solution for lipids visualization (upper right panel). Comparison between the intensity of the bands observed in the LPS profiles of the wt and the Δ*sigF* mutant (lower panel) (** p value ≤ 0.01).

Fig. 6. Negatively stained transmission electron micrographs of *Synechocystis* wild-type and Δ*sigF*. **A.** cells. **B.** 500x concentrated cell-free media. The presence of vesicles (vs) and pili (black arrowheads) is depicted for the wt, whereas for Δ*sigF* a dense layer surrounding the cell (white arrowheads). **C.** Directional motility agar assay showing the phototaxis of wt and the non-motile phenotype of Δ*sigF*. Dashed circles indicate the place where cell culture was spotted.

Fig. 7. Exoproteomes of *Synechocystis* wild-type and Δ*sigF* separated by SDS-PAGE/stained with Coomassie Blue. Numbers to the right highlight the bands/gel region observed across at least three biological replicates and excised for protein identification (**Table 2**).

Fig. 8. Functional groups of proteins encoded by genes with putative SigF binding motifs in the promoters. See annotated list of genes in Supporting Information Table S3.

Fig. 9. Functional groups of proteins with significant fold changes in *Synechocystis* Δ*sigF* *vs.* wild-type. **A**. Distribution by functional categories of the total number of proteins quantified in the iTRAQ analysis. **B.** Number of proteins in each functional category with significant higher or lower abundance in Δ*sigF* compared to the wild-type. See annotated list of proteins in Supporting Information Table S4.

Fig. 10. Schematic representation of *Synechocystis* Δ*sigF* phenotype/genotype. Both classical and non-classical secretion pathways are altered in the mutant. EPS: extracellular polymeric substances, OM: outer membrane, PG: peptidoglycan, IM: inner membrane, T4SS: type 4 secretion system, T1SS: type 1 secretion system, RND pump: resistance-nodulation-division pump.

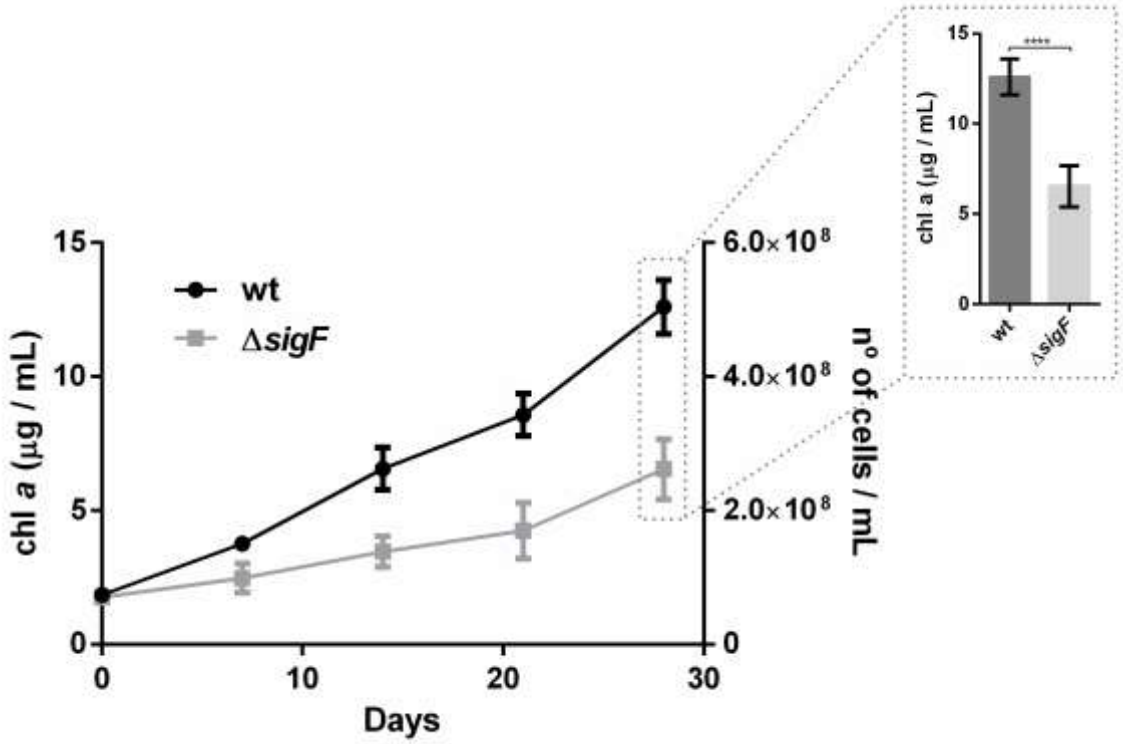

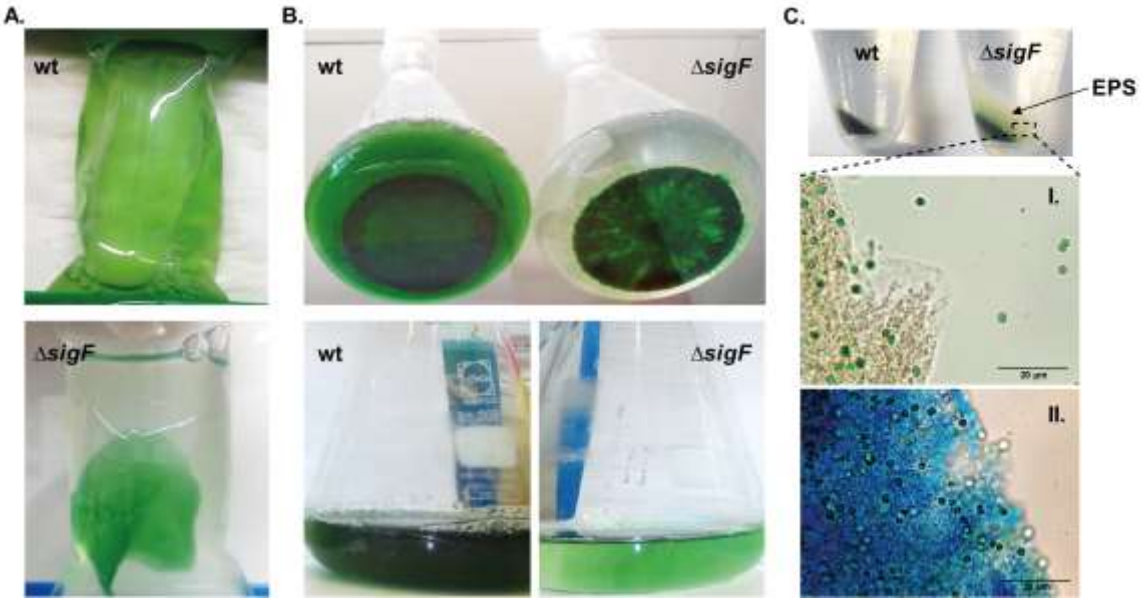

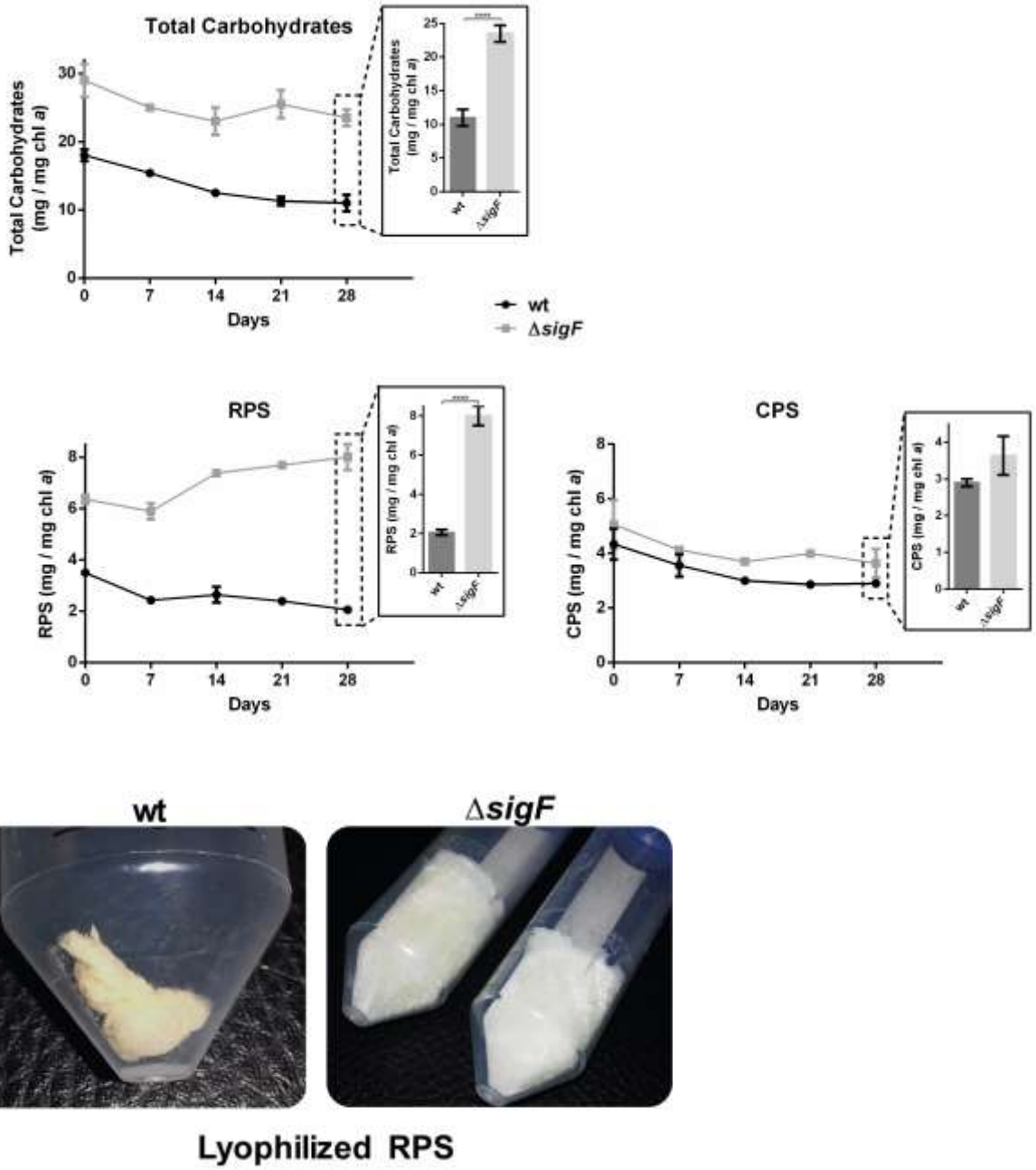

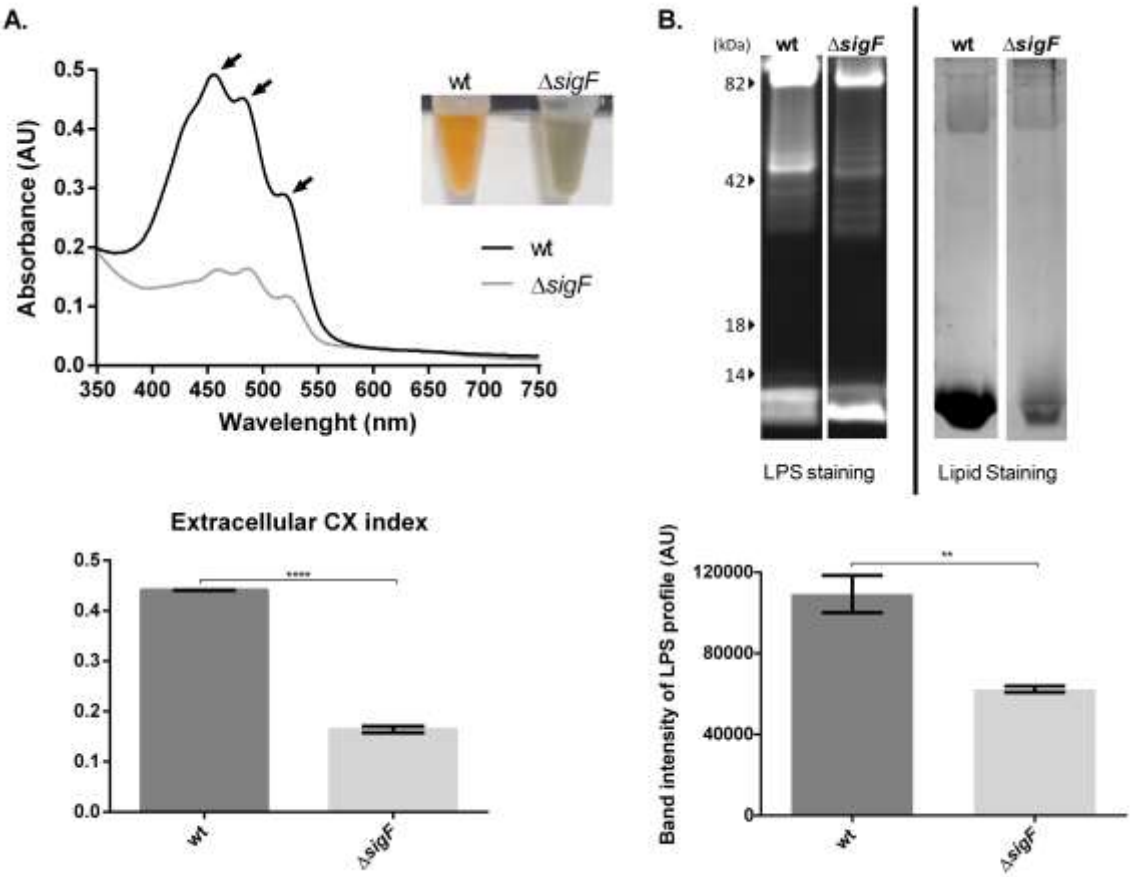

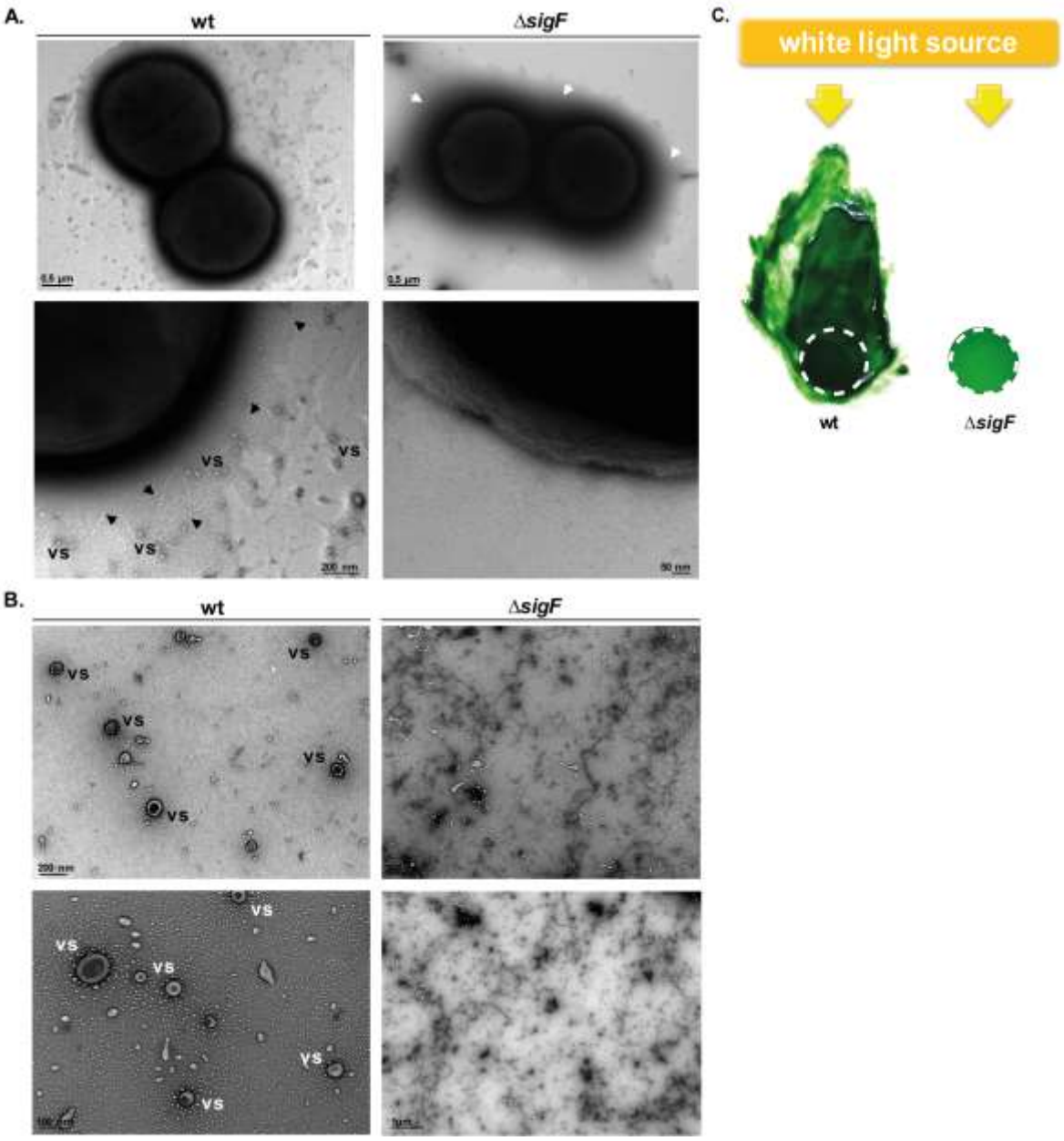

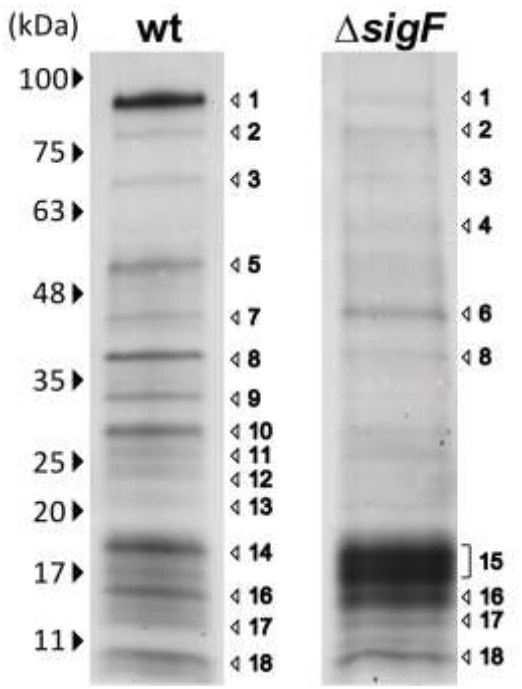

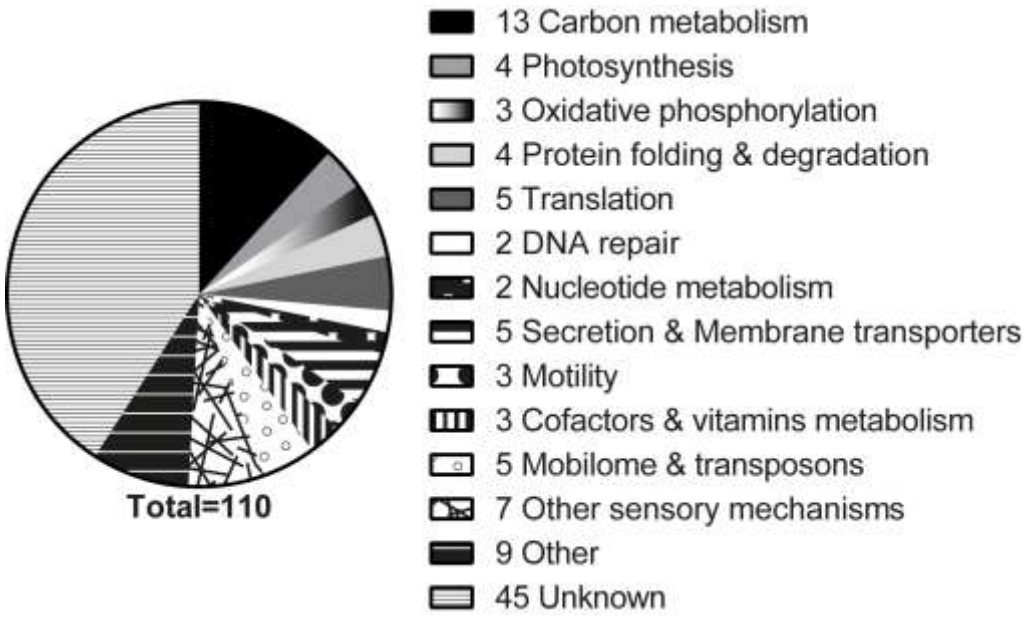

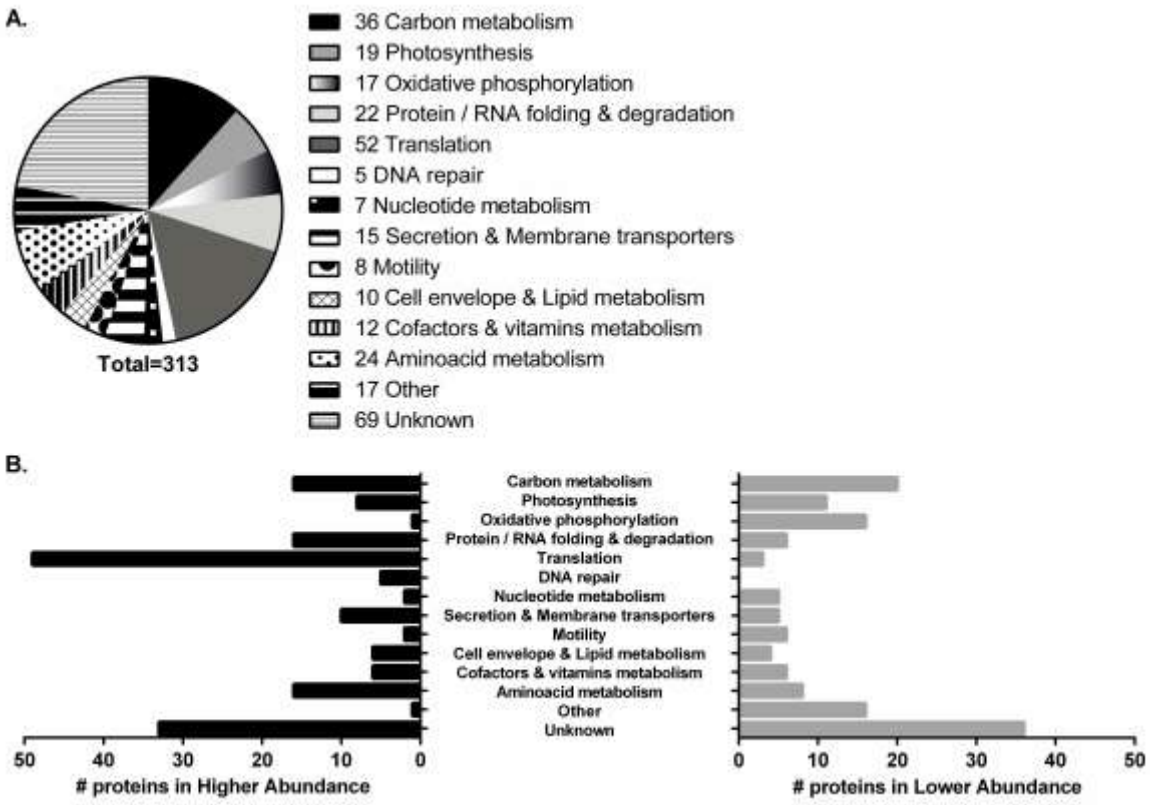

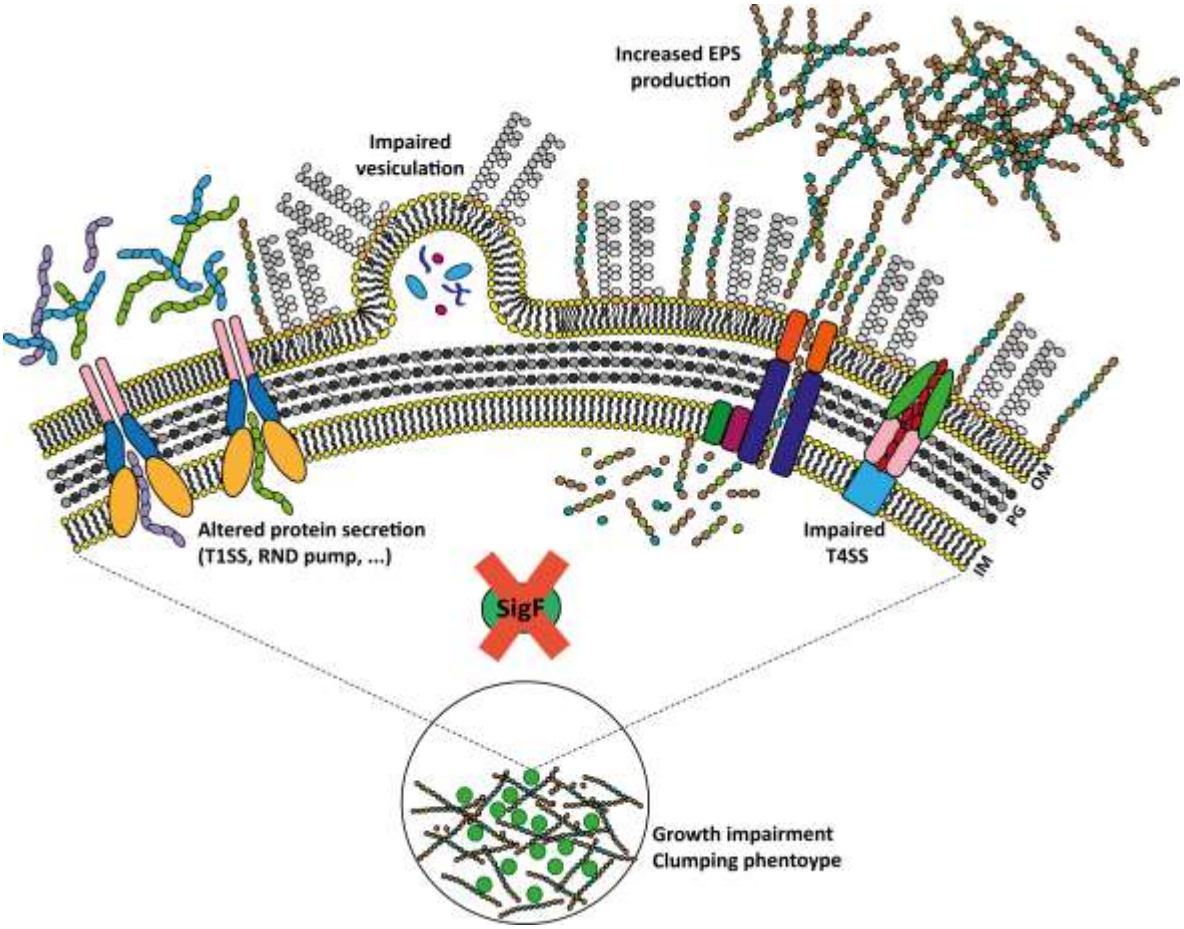

Table 1. Monosaccharidic composition of the RPS obtained from *Synechocystis* wild-type and Δ*sigF* cultures expressed as molar %.

	wt		**Δ*sigF***	
Monosaccharide	**Mean**	**SD**	**Mean**	**SD**
Glucose	18.54	0.94	33.87	1.50
Mannose	17.74	0.70	20.29	0.45
Galactose	2.53	0.53	5.03	0.60
Rhamnose	14.24	1.56	17.23	0.35
Fucose	10.28	0.16	3.89	0.41
Xylose	6.05	0.11	5.73	0.52
Arabinose	1.83	0.57	Traces	-
Ribose	1.35	0.02	Traces	-
Glucosamine	12.42	1.36	5.17	0.43
Galactosamine	9.34	0.78	4.13	0.15
Glucuronic acid	4.16	0.74	1.35	0.22
Galacturonic acid	Traces	-	1.76	0.04

Table 2. List of proteins identified in the exoproteomes of *Synechocystis* sp. PCC 6803 wild-type (wt) and Δ*sigF* mutant by mass spectrometry.

Band	Protein	Description
1	**Sll1009,** FrpC	Protein with calcium ion binding motifs
2	**Slr0168**	Unknown
3	**Slr1841**	Porin (carbohydrate selective)
4	**Slr0191,** SpoIID	Amidase enhancer, role at murein and peptidoglycan
5	**Slr0447,** AmiC & **Slr1940**	ABC transporter (urea) & prot. involved in extracellular connection structures
6	**Slr1751,** PrC & **Sll1525,** PrK	protease (PSII repair) & CO_2 fixation
7	**Slr1452** SbpA	Sulfate transport
8	**Slr0513,** FutA	Iron uptake (PSII protection from ROS)
9	**Slr1410** & **Sll1491**	WD proteins
10	**Sll0314**	Lipoprotein (signaling)
11, 12, 13	**Slr1704**	Unknown
14	**Sll1577,** CpcB	C-phycocyanin beta chain
15	**Sll1578,** CpcA & **Slr2067,** ApcA & **Sll1577**	C-phycocyanin alpha chain & Allophycocyanin alpha chain
16	**Slr0518**	Carbohydrate binding protein (arabinofuranidase)
17	**Sll0470**	Unknown
18	**Sll1029** & **Sll1028**	CCMK (CO_2 concentrating mechanism)

Table 3. List of proteins displaying significant fold changes in *Synechocystis* Δ*sigF* compared to the wild-type (A and B are the two iTRAQ studies), encoded by genes displaying putative SigF binding motifs in their promoter regions.

Protein name	Uniprot ID	Description	Functional Category	Fold changes (mt : wt)	
				A	B
Slr1301	P72839	Predicted ABC transporter	Unknown	2,05	2,06
Sll1127, MenB	P73495	DHNA-CoA synthase	Cofactors & vitamins metabolism	1,12	-
Sll1812, RpsE, Rps5	P73304	30S ribosomal protein S5	Translation	1,28	1,23
Slr1837	P73107	Predicted UDP-dehydrogenase	Unknown	-	1,16
Sll1654	P72817	Universal stress protein	Unknown	-	1,22
Slr1338	P74074	Hypothetical protein	Unknown	1,30	1,22
Sll0634, BtpA	P72966	Protein involved in PSI biogenesis	Photosynthesis	1,20	1,18
Slr1525, PrK, Ptk	P37101	Phosphoribulokinase	Carbon metabolism	2,00	2,16
Slr0884, Gap1	P49433	Glyceraldehyde-3-phosphate dehydrogenase 1 (GAPDH 1)	Carbon metabolism	-1,50	-1,60
Sll0837	P73762	Periplasmic protein similar to TadD (Pilus assembly protein)	Unknown	-1.35	-
Sll1694, HofG	P73704	General secretion pathway protein G	Motility	-2,27	-2,39
Ssl3093, CpcD	P73202	Phycobilisome rod-linker polypeptide	Photosynthesis	-1,34	-1,40